Journal of Inorganic and General Chemistry
ZAAC
Zeitschrift für anorganische und allgemeine Chemie
DOI: 10.1002/zaac.201900228
ARTICLE

Polyanionic Frameworks in the Lithium Phosphidogermanates Li_2GeP_2 and $LiGe_3P_3$ – Synthesis, Structure, and Lithium Ion Mobility

Henrik Eickhoff,[a] Christian Sedlmeier,[a] Wilhelm Klein,[a] Gabriele Raudaschl-Sieber,[a] Hubert A. Gasteiger,[a] and Thomas F. Fässler*[a]

Dedicated to Professor Hans-Jörg Deiseroth on the Occasion of his 75th Birthday

Abstract. Recently fast lithium ion conductors were discovered in compounds containing tetrahedral SiP_4^{8-} and GeP_4^{8-} units. In the context of material development for all solid state batteries the ternary Li/Ge/P phase system has been further investigated and two new lithium phosphidogermanates were discovered on the lithium poor side of the ternary composition diagram. Li_2GeP_2 crystallizes in space group $I4_1/acd$ with unit cell parameters of a = 12.3069(1) Å and c = 19.0306(4) Å, consists of a framework of Ge_4P_{10} supratetrahedra, and exhibits an ionic conductivity of $1.5(3)\times10^{-7}$ S·cm^{-1} at 27 °C. $LiGe_3P_3$ crystallizes in *Pbam* with a = 9.8459(5) Å, b = 15.7489(7) Å, and c = 3.5995(2) Å. In $LiGe_3P_3$ Ge and P atoms form a two dimensional polyanion. The slabs consist of five- and six-membered heteroatomic rings comprising GeP_4 and $Ge(P_3Ge)$ tetrahedra including homoatomic Ge–Ge bonds. A semiconducting behavior with an electronic conductivity of ~10^{-4} S·cm^{-1} and a remarkable stability vs. air and moisture is observed.

Introduction

The ongoing research on all solid state batteries as a next generation battery type is accompanied by the development of new materials. Especially, for the application as solid electrolytes a broad spectrum of compounds has been investigated.[1,2] Oxide based ion conductors are one of the largest groups and show generally good electrochemical compatibility with electrodes but relatively low ionic conductivities.[3,4] To overcome this drawback oxide was substituted with the larger and softer sulfide leading to very promising LGPS-type compounds and Li-argyrodites exhibiting conductivities larger than 1 mS·cm^{-1}.[5,6] Recently, in an attempt to further increase the ionic conductivity phosphides have been investigated. The phosphide ion exhibits a higher charge compared to oxide and sulfide leading to an increased charge carrier concentration. These efforts resulted in the development of lithium phosphidotetrelates – named for their structural similarity to oxidosilicates – Li_8SiP_4, Li_2SiP_2, $LiSi_2P_3$, and α- and β-Li_8GeP_4, which show conduction values of up to 0.1 mS·cm^{-1}.[7–9]

Despite the alternating composition, lithium phosphidosilicates consist of tetrahedral building blocks also found in conventional fast ion conductors. Therefore, a close relationship to the above mentioned conventional solid electrolytes containing PS_4^{3-} and GeS_4^{4-} is present. Recently, even the relationship to Deiseroth's lithium argyrodites was established. In argyrodites S^{2-} ions appear beside the tetrahedral PS_4^{3-} units and in accordance the reported $Li_{14}SiP_6$ contains two P^{3-} anions per SiP_4^{8-} tetrahedral unit.[10]

With respect to structure chemistry can the SiP_4^{8-} units in ortho phosphidosilicates Li_8SiP_4 undergo – in analogy to ortho oxo-silicate – formally condensation reactions resulting in vertex- or edge-sharing tetrahedra. In consequence dimeric units are observed in $Li_{10}Si_2P_6$,[11] polyanionic layers in $Li_3Si_3P_7$[11] and three dimensional networks in Li_2SiP_2[7] and $LiSi_2P_3$.[8]

For compounds containing heavy *A* and *Pn* elements a larger number of crystal structures containing also homoatomic tetrel-tetrel bonds and formally negatively charged tetrel atoms are reported such as $K_6Sn_3As_5$ and KSnAs[12] which are so far not reported for ternary Li/Si/P compounds. A further frequently occurring composition is ATt_3Pn_3 (*A* = Li, Na, K, Rb: *Tt* = Si, Ge, Sn; *Pn* = P, As).[13–15] whose structures consist of *Tt*–*Pn* slabs, which are separated by *A* atoms. In the cross section the slabs appear as columns of pentagonal rings bridged with attached *Pn* atoms (Figure 1). The rings represent tubes built from 9 atom cages or, from a different point of view, corner sharing $TtPn_4$ tetrahedra connected via Tt_2 dumbbells. Various stacking orders of the slabs lead to diverse structure types. The structural flexibility of this system is also exhibited by KSi_3As_3,[16] in which certain *Tt* and *Pn* positions are swapped, leading to a different connectivity of the tubes, and by Li_3NaSi_6,[17] in which the slabs are solely built from Si.

* Univ.-Prof. Dr. Thomas F. Fässler
E-Mail: Thomas.Faessler@lrz.tu-muenchen.de
[a] Department of Chemistry
Technische Universität München
Lichtenbergstraße 4
80333München, Germany
Supporting information for this article is available on the WWW under **http://dx.doi.org/10.1002/zaac.201900228** or from the author.

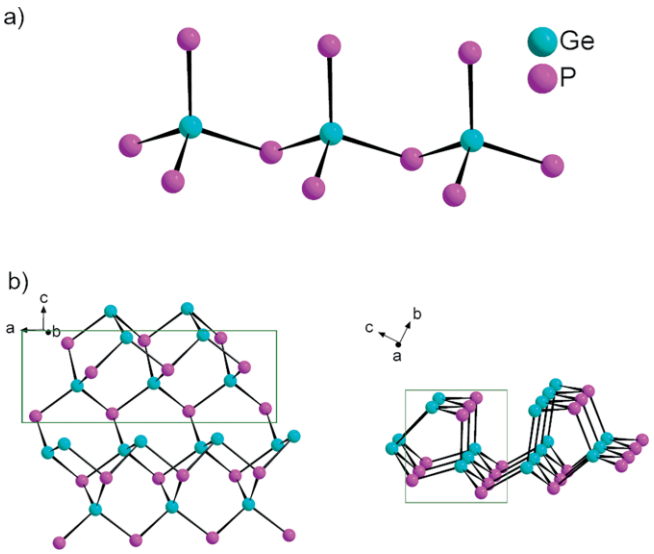

Figure 1. (a) Chain of GeP_4 tetrahedra. (b) Section of polyanionic slabs found in $NaGe_3P_3$ with view from different directions. Green boxes highlight GeP_4 tetrahedra chains.

While various compounds are known for the heavier homologues and also lithium phosphidosilicates, the intermediate lithium phosphidogermanates are sparsely investigated. With α-Li_8GeP_4 and β-Li_8GeP_4 this system has been shown to realize structure types same as found for light (Li_8SiP_4) and heavy tetrel elements (Li_8SnP_4), respectively.[6] Beside α-Li_8GeP_4 and β-Li_8GeP_4 the only further compound reported is Li_5GeP_3, crystallizing in the CaF_2 structure type.[18] Thus the so far known compounds consist exclusively of isolated GeP_4 tetrahedra. Regarding the structural diversity of the related phase systems many more compounds are conceivable. Additionally, as already seen for the α-Li_8GeP_4 and β-Li_8GeP_4 the substitution of Si by Ge can lead to alternating properties, like increased or decreased ionic conductivity depending on the crystal structure.

In this context the Li/Ge/P phase system is further explored and the new lithium phosphidogermanates Li_2GeP_2 and $LiGe_3P_3$ are presented.

Results and Discussion

Li_2GeP_2

Almost single phase microcrystalline material of Li_2GeP_2 is obtained by ball milling and subsequent annealing at 600 °C. Single crystals of Li_2GeP_2 for crystal structure analysis are obtained from a stoichiometric reaction of the elements in a Ta ampoule at 700 °C. In the product mixture Li_2GeP_2 was found beside Ge and $LiGe_3P_3$. The new compound crystallizes with space group $I4_1/acd$ and unit cell parameters $a = b =$ 12.30697(14) Å and $c =$ 19.0307(4) Å (120 K) (Table 1). Li_2GeP_2 is isotypic to known Li_2SiP_2.[7] The structure contains one crystallographic position for Ge and three independent positions for P and Li, respectively. All P atoms form a strongly distorted cubic closed packing with Li and Ge atoms in slightly distorted tetrahedral voids. As a result, every Ge atom is covalently bound to four P atoms, one P1 (Wyckoff pos. 16*d*), one P2 (16*e*) and two P3 (32*g*), forming tetrahedral GeP_4 units. Ge-P distances are in the range of 2.3147(5) to 2.3445(4) Å, and are slightly shorter than the Ge–P bonds in α- and β-Li_8GeP_4 [*d*(Ge–P) of 2.369–2.405 Å]. Four tetrahedra are condensed via common corners and form supertetrahedra which are further connected via shared corners to a hierarchical variant of a diamond structure. In the crystal structure two interpenetrating networks are present (Figure 2).

Table 1. Refinement data of the single crystal diffraction data of Li_2GeP_2 and $LiGe_3P_3$ at 120 K.

	Li_2GeP_2	$LiGe_3P_3$
Molar mass /g·mol^{-1}	148.458	317.751
Crystal system	tetragonal	orthorhombic
Space group	$I4_1/acd$ (142)	Pbam (55)
Radiation λ /Å	0.71073 (Mo-K_α)	0.71073 (Mo-K_α)
Crystal size /mm^3	0.40 × 0.21 × 0.19	0.55 × 0.07 × 0.01
Crystal color, shape	red, block	black, bar
Cell parameters		
a /Å	12.30697(14)	9.8459(5)
b /Å	12.30697(14)	15.7489(7)
c /Å	19.0307(4)	3.5995(2)
Cell volume /Å^3	2882.42(9)	558.15(5)
Z	32	4
ρ (calcd.) /g·cm^{-3}	2.736	3.780
μ /mm^{-1}	9.109	16.750
F(000)	2176	576
Temperature /K	120	120
Reflections collected	22367	6903
Independent reflections	1057	927
Reflections with $I > 2\sigma(I)$	967	733
Observed *hkl*	$-17 \le h \le 17$ $-17 \le k \le 17$ $-26 \le l \le 26$	$-13 \le h \le 13$ $-21 \le k \le 22$ $-5 \le l \le 5$
Measuring range $\theta_{min/max}$ /°	3.17 / 29.99	3.31 / 30.00
Goodness-of-fit on F_o^2	1.115	0.986
R_{int} / R_σ	0.0326 / 0.0123	0.0524 / 0.0362
R indices [$F_0^2 \le 2\sigma(F_o^2)$]	*R*1 = 0.0120 *wR*2 = 0.0283	*R*1 = 0.0306 *wR*2 = 0.0757
R indices (all data)	*R*1 = 0.0141 *wR*2 = 0.0287	*R*1 = 0.0409 *wR*2 = 0.0775
Largest diff. peak/hole /e·Å^{-3}	0.37 / –0.35	1.44 / –1.09

While all Ge atoms are coordinated by 4 P atoms, all P atoms bridge Ge atoms (Table 2). Two-fold connected P atoms result in a formal charge of –1 per P atom. The negative charge is balanced by Li atoms that occupy the pseudo tetrahedral voids of the *ccp* of P atoms between the frameworks. The resulting coordination sphere for all P atoms consists of four Li^+ beside the two Ge atoms. Li–P distances in Li_2GeP_2 are in the range of 2.548(4)–2.738(1) Å and are thus significantly longer than in Li_2SiP_2 [*d*(Li–P) = 2.444(2)–2.767(2) Å; Table 3].

To confirm the crystal structure and purity, ^{31}P-MAS-NMR spectra were recorded. The number and intensity of the observed signals agrees well with the crystallographic data. Three signals with a chemical shift of δ = –59.9, –164.8, –178.4 ppm and a relative intensity of 1:1:2 are assigned to the P positions

Table 2. Atom coordinates of Li_2GeP_2 at 120 K from single crystal diffraction data.

Atom	Wyck.	x	y	z	U_{iso}
Ge1	32*g*	0.38142(2)	0.33808(2)	0.05570(2)	0.00636(5)
P1	16*d*	0.5000	0.2500	–0.02212(3)	0.00768(10)
P2	16*e*	0.2500	0.44300(4)	0.0000	0.00714(9)
P3	32*g*	0.28249(3)	0.22328(3)	0.12775(2)	0.00793(7)
Li1	16*f*	0.0946(2)	0.1554(2)	0.1250	0.0148(7)
Li2	16*f*	0.1563(2)	0.4063(2)	0.1250	0.0186(8)
Li3	32*g*	0.3746(2)	0.0991(2)	0.03521(13)	0.0156(5)

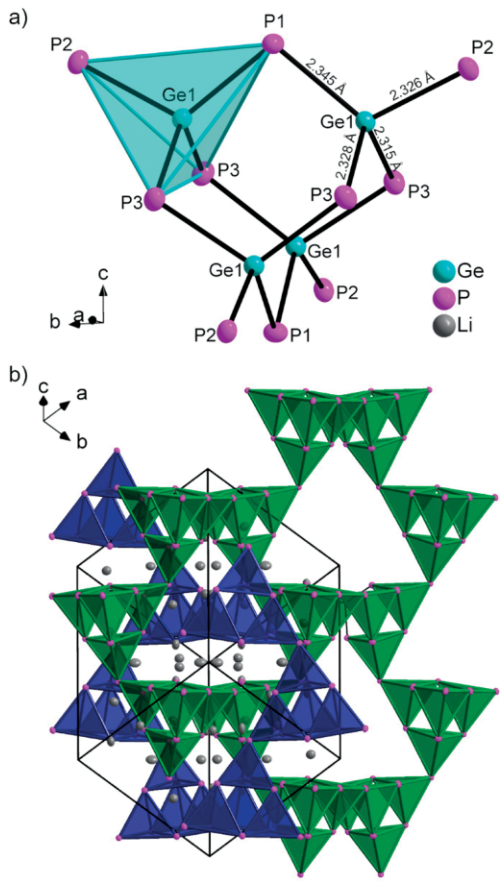

Figure 2. Structural features of Li_2GeP_2. (a) A covalently bound Ge_4P_{10} supertetrahedron with bond lengths. A single GeP_4 tetrahedron is highlighted in light blue. (b) The unit cell with the two independent diamond like frameworks of supertetrahedra depicted in dark blue and green.

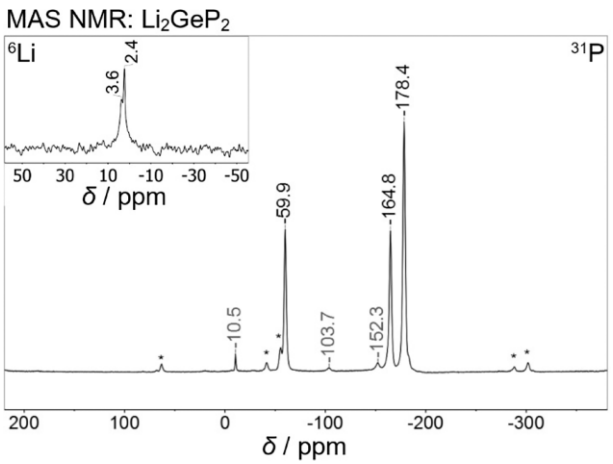

Figure 3. ^{31}P MAS NMR spectrum of Li_2GeP_2 with inset for ^6Li MAS NMR spectrum. Signals from side phases are indexed with grey colored chemical shifts and rotation side bands are marked with asterisks.

P2, P1 and P3, respectively (Figure 3). The strong downfield chemical shift of P2 is attributed to the more different chemical environment. This atom represents the shared corner of condensed supertetrahedra, while P1 and P3 are situated on the edges of the supertetrahedra, therefore exhibiting a very similar chemical environment. All P atoms are surrounded by two Ge atoms and four Li atoms. While the coordination sphere of Li atoms does not show features explaining the differences between the three P sites, the Ge–P–Ge bond angle is for P2 significantly larger (112.5°) compared to P1 (101.7°) and P3 (105.0°).

In isotypic Li_2SiP_2 only two strongly upfield shifted NMR signals at δ = –129.1 and –241.5 ppm) with a relative intensity of 1:3 are observed.[7] These two signals are assigned to P2 and a not resolved peak for P1 and P3, respectively. The splitting of the P1 and P3 signal in Li_2GeP_2 can be attributed to more expressed differences in bond angles of the atoms connected to the P atoms. While the local coordination of all P atoms within Li_2GeP_2 and Li_2SiP_2 through *Tt* atoms is very similar, a stronger deviation of *Tt*–P–*Tt* bond angles from the ideal tetrahedral angle is observed in Li_2GeP_2. The deviation in Li_2GeP_2, with a Ge–P–Ge angle of 101.7° at P1 and 105.0° at P3 is much larger than in Li_2SiP_2 (103.0° and 105.1°), respectively.[7]

Along the four equivalent [111] directions of the cubic crystal system the tetrahedra framework bears large three-dimensionally connected channels that are occupied by Li^+. In combination with only two signals found in ^6Li MAS NMR (δ = 2.4 ppm, 3.6 ppm) for three different crystallographic Li sites.

For an estimation of the ion conduction potential of Li_2GeP_2 geometric parameters are compared with those from the silicon containing compound. As expected the shortest Li–Li distances within the channels increase slightly with substitution of Si by Ge from a range of 2.916(9)–3.229(9) Å to 2.940(5)–3.290(5) Å, respectively. In contrast to the increasing Li-Li distances and unit cell parameters the bottle neck size, indicated by shortest P–P distances within the channel, shrinks, due to a rotation and distortion of the supertetrahedra. As a consequence two different occurring P–P distances decrease from 3.954(2) Å and 4.0012(9) Å to 3.9161(8) Å and 3.978(5) Å. Both effects might be responsible for the lower ionic conduc-

Table 3. Selected distances and angles in Li_2GeP_2 at 120 K from single crystal diffraction data.

Atom 1	Atom 2	d_{1-2} /Å		Atom 1		Atom 2		Atom 3	Angle
Ge1	P3	2.3147(5)		P3	–	Ge1	–	P2	104.07(1)
Ge1	P2	2.3258(4)		P3	–	Ge1	–	P3	110.54(1)
Ge1	P3	2.3280(5)		P2	–	Ge1	–	P3	101.86(2)
Ge1	P1	2.3445(4)		P3	–	Ge1	–	P1	114.79(1)
Ge1	Li3	2.969(3)		P2	–	Ge1	–	P1	113.69(1)
Ge1	Li3	3.083(3)		P3	–	Ge1	–	P1	110.97(1)
Ge1	Li3	3.124(4)		Ge1	–	P2	–	Ge1	112.51(3)
Ge1	Li2	3.179(2)		Ge1	–	P1	–	Ge1	101.66(2)
P1	Li1	2.557(3)	2×	Ge1	–	P3	–	Ge1	104.99(2)
P1	Li3	2.653(3)	2×						
P2	Li3	2.548(4)	2×						
P2	Li2	2.679(2)	2×						
P3	Li1	2.460(2)							
P3	Li3	2.590(3)							
P3	Li3	2.626(4)							
P3	Li2	2.738(1)							
Li1	Li2	3.184(5)	2×						
Li1	Li3	3.155(4)	2×						
Li1	Li1	3.29(1)							
Li2	Li3	2.941(4)	2×						
Li3	Li3	3.353(7)							

tivity of $1.5(3) \times 10^{-7}$ S·cm^{-1} in Li_2GeP_2 at 27 °C compared to 4×10^{-7} S·cm^{-1} in Li_2SiP_2 at 25 °C.[7] However, the measured conductivity is a combination of bulk and grain boundary (C = 0.34–0.39 nF; ω_{Apex} = 510–860 kHz; $\alpha \geq 0.99$) and since the two contributions were not resolved in the impedance spectrum cannot exclusively be interpreted by contribution of the structural changes. The electronic contribution of 10^{-8} S·cm^{-1} to the conductivity is only minor and in the same order of magnitude as reported for Li_2SiP_2.[7]

$LiGe_3P_3$

4The second new compound, $LiGe_3P_3$, is prepared as almost single phase microcrystalline material via ball milling and subsequent annealing at 500 °C. Single crystals of $LiGe_3P_3$ are obtained through a stoichiometric reaction of the elements in a sealed Ta ampoule at 700 °C. The resulting product contained $LiGe_3P_3$, Ge, and Li_3P_7 as a result of the different chosen sample composition of $Li_3Ge_3P_7$ and the high melting point of Ge. $LiGe_3P_3$ crystallizes in the orthorhombic space group *Pbam* with the unit cell parameters of a = 9.8459(5) Å, b = 15.7489(7) Å and c = 3.5995(2) Å (120 K) (Table 1). The second new compound, $LiGe_3P_3$ is isotypic to $Li_{0.9}Ge_{2.9}As_{3.1}$[14] and comprises similar building blocks known from other compounds of the heavier homologues such as $NaGe_3P_3$.[13] Three crystallographic independent of each Ge and P atoms positions form a covalently connected two-dimensional polyanion that are separated in layers by Li (Table 4). As shown in Figure 4 Ge1 and all P sites form chains of corner-sharing GeP_4 tetrahedra. These are a reoccurring structural motive in phosphidogermanates.

The linear arrangement of GeP_4 tetrahedra along the c axis allows the formation of two six-membered rings between neighboring tetrahedra by the addition of two additional Ge atoms (Ge2 and Ge3) ({P2–Ge1–P3–Ge2–P3'–Ge1'} and {P2–Ge1–P1–Ge3–P1'–Ge1'}). The rings are further interconnected by a Ge2–Ge3 bond. As a consequence to further five-membered rings of the same atom sequence {Ge1–P1–Ge3–Ge2–P3} result.

Additionally, this connectivity pattern leads to the formation of a second type of tetrahedra, Ge(P_3Ge), which is – due to the different atom types – strongly distorted. These tetrahedra are connected to GeP_4 tetrahedra by sharing a P vertex and forming one *exo*-tetrahedral Ge2–P3 bond.

This connectivity pattern leads to the formation of quasi pentagonal tubes parallel to the c axis. Further bonds between P2 atoms to Ge3 atoms of the neighboring tubes result in two dimensional sheets in the *ac* plane. Within these slabs, all P atoms are connected to three Ge atoms, leading to a formal charge of 0.

Table 4. Atom coordinates of $LiGe_3P_3$ at 120 K from single crystal diffraction data.

Atom	Wyck.	x	y	z	U_{iso}
Ge1	4 *g*	0.38362(7)	0.14362(4)	0.0000	0.0084(2)
Ge2	4*h*	0.05770(7)	0.10283(4)	0.5000	0.0121(2)
Ge3	4*h*	0.15069(7)	0.25321(4)	0.5000	0.0092(2)
P1	4 *g*	0.3006(2)	0.28278(10)	0.0000	0.0093(3)
P2	4*h*	0.5277(2)	0.11779(10)	0.5000	0.0087(3)
P3	4 *g*	0.1987(2)	0.05294(10)	0.0000	0.0100(3)
Li1	4*h*	0.7931(13)	0.0699(9)	0.5000	0.025(3)

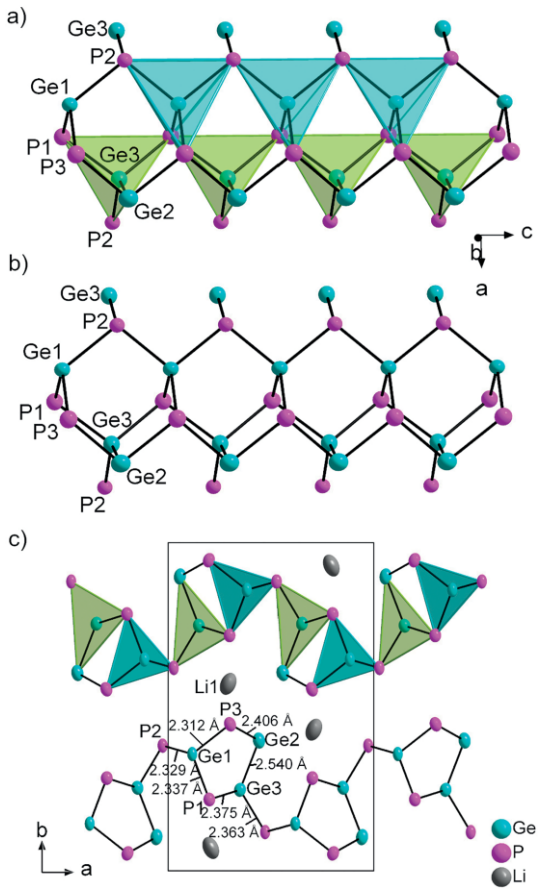

Figure 4. Structural features of $LiGe_3P_3$. (a) Detailed view of a Ge_3P_3 tube consisting of corner sharing GeP_4 tetrahedra (light blue) and GeP_3Ge tetrahedra (green). (b) Detailed view of a Ge_3P_3 tube without highlighted tetrahedra. (c) Expanded unit cell with slabs of Ge-P tubes. Tetrahedra are highlighted to emphasize the conductivity.

The atoms Ge1 and Ge3 form four covalent bonds to four P atoms or to three P atoms and one Ge atom, respectively. Since Ge2 is threefold connected to two P and one Ge atom a formal charge of –1 results. The negative charge of the polyanion is balanced by one Li ion per formula unit, thus $LiGe_3P_3$ is a charge balanced compound. Interestingly, $LiGe_3P_3$ is the first lithium phosphidotetrelate comprising formally charge neutral P atoms and a negatively charged Ge atom.

The Ge–P distances occurring in this compound of 2.314(2)–2.405(1) Å are in the range of typical Ge–P single bonds (Table 5). With a length of 2.5391(9) Å the Ge–Ge single bonds are longer than those in elemental Ge (2.450 Å)[19] and GeP (2.369, 2.393 Å)[20] but significantly shorter than in $NaGe_3P_3$ (2.627 Å).[13]

The Li atom is situated in a strongly distorted tetrahedral coordination of three P [d(Li–P) = 2.64(1)–2.94(1) Å] and one Ge [d(Li–Ge) = 2.66(1) Å]. In the second coordination sphere the distorted tetrahedron is supplemented by two P atoms and two Ge atoms to a two times capped, heavily distorted octahedron.

Impedance spectroscopy and polarization measurements hint for a dominant electronic conduction of approximately 10^{-4} S·cm^{-1} (C = 0.40–0.49 nF; ω_{Apex} = 160–300 kHz; $\alpha \geq 0.99$) and no ionic share could be detected. The value is the highest reported electronic conductivity of lithium phosphidogermanates so far.

^{31}P MAS NMR spectra confirm the crystallographic results (Figure 5). Three signals occur within a small chemical shift range (δ = –59.5, –119.4, –126.3 ppm) and an intensity ratio of 1:1:1. According to only one independent crystallographic site for Li, in the ^{6}Li MAS NMR spectrum a single signal at δ = 2.4 ppm is detected.

Syntheses

Almost single phase bulk material of Li_2GeP_2 and $LiGe_3P_3$ is prepared from a two-step synthesis route, including mechanochemical milling and subsequent annealing. The mechanical processing reduces grain sizes, improves the distribution of elements and, additionally, leads to the formation of precursor compounds in a reactive mixture. Temperatures of 600 °C and 500 °C, respectively, applied in the following annealing step are chosen based on DSC measurements. For Li_2GeP_2 an onset for melting and solidifying is observed between 684 °C and

Table 5. Selected distances and angles in $LiGe_3P_3$ at 120 K from single crystal diffraction data.

Atom 1	Atom 2	d_{1-2} /Å		Atom 1		Atom 2		Atom 3	Angle
Ge1	P3	2.314(2)		P3	–	Ge1	–	P2	111.82(5)
Ge1	P2	2.328(1)	2×	P2	–	Ge1	–	P2	101.29(7)
Ge1	P1	2.339(2)		P3	–	Ge1	–	P1	107.66(6)
Ge2	P3	2.405(1)	2×	P2	–	Ge1	–	P1	112.13(5)
Ge2	Ge3	2.5391(9)		P3	–	Ge2	–	P3	96.90(6)
Ge2	Li1	2.66(1)		P3	–	Ge2	–	Ge3	95.54(4)
Ge2	Li1	3.09(1)		P2	–	Ge3	–	P1	98.62(5)
Ge3	P2	2.365(2)		P1	–	Ge3	–	P1	98.60(6)
Ge3	P1	2.374(1)	2×	P2	–	Ge3	–	Ge2	128.07(5)
Ge3	Li1	3.12(1)		P1	–	Ge3	–	Ge2	114.03(4)
P1	Li1	2.94(1)	2×	Ge1	–	P1	–	Ge3	91.92(5)
P2	Li1	2.72(1)		Ge3	–	P1	–	Ge3	98.60(6)
P3	Li1	2.64(1)	2×	Ge1	–	P2	–	Ge1	101.29(7)
				Ge1	–	P2	–	Ge3	99.32(5)
				Ge1	–	P3	–	Ge2	104.63(5)
				Ge2	–	P3	–	Ge2	96.90(6)

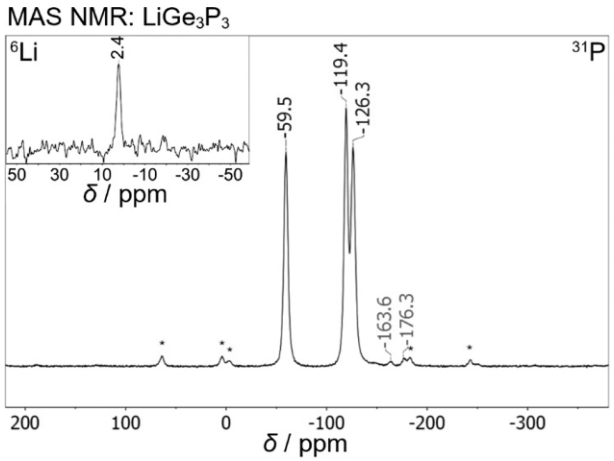

Figure 5. ^{31}P MAS NMR spectrum of $LiGe_3P_3$ with inset for ^{6}Li MAS NMR spectrum. Signals from side phase Li_2GeP_2 are indexed with grey colored chemical shifts and rotation side bands are marked with asterisks.

677 °C, respectively. In $LiGe_3P_3$ these thermal events are assigned to distinct peaks is observed with onsets of 701 °C and 647 °C. All samples were synthesized with an excess of 5–7 % Li. Compared to stoichiometric mixtures this excess reduces the phase fraction of side phases, especially unreacted Ge, in the final product. Following that approach phase fractions can be determined via Rietveld refinement (Figure 6) to be 97 % for $LiGe_3P_3$, containing 1 % Ge and 2 % Li_2GeP_2.

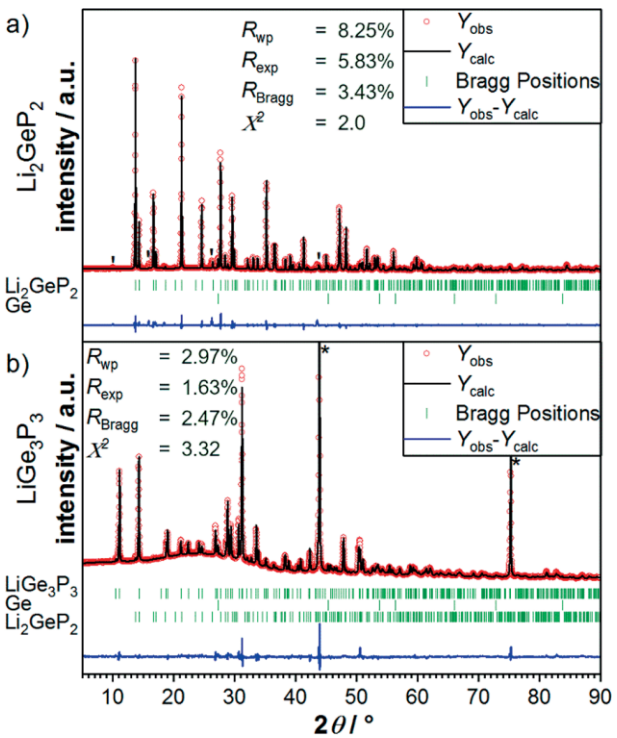

Figure 6. Rietveld refinement plots of (a) Li_2GeP_2 and (b) $LiGe_3P_3$ samples. Y_{obs} is the observed and Y_{calc} the calculated intensity. The unknown side phase in Li_2GeP_2 is marked with ticks (‘) and added diamond powder reflection with asterisks (*) and are truncated for better visualization of the sample reflections.

Since additional reflections occur in the diffraction pattern of Li_2GeP_2 which cannot be assigned to a known compound, an exact determination of the phase fractions is not possible. Comparison of the Li_2GeP_2 and Ge content leads to a ratio of 86:1. While Li_2GeP_2, similar to all other known lithium phosphidogermanates and lithium phosphidosilicates, shows vigorous reactions in contact with water, $LiGe_3P_3$ exhibits a remarkable stability. By deliberately exposing $LiGe_3P_3$ samples to air and water for 24 h each, followed by PXRD measurements, no change in crystallinity and ratio of $LiGe_3P_3$ and Ge is detected, while the Li_2GeP_2 side phase clearly degrades. This stability against moisture may be explained by structural features of $LiGe_3P_3$, as there are the low charge of the anionic partial structure together with a higher degree of condensation of GeP_4 units.

Conclusions

The new lithium phosphidogermanates Li_2GeP_2 and $LiGe_3P_3$ are the first compounds with large polyanions in the Li/Ge/P phase system and comprise three- and two-dimensional anionic substructure, respectively. The realized structure types are known for lighter and heavier homologues, respectively, and both contain GeP_4 units, which are a common building block for all lithium phosphidotetrelates. In Li_2GeP_2, which is isotypic to Li_2SiP_2, the tetrahedra form frameworks of Ge_4P_{10} supertetrahedra and large channels for Li^+. In contrast to the increasing unit cell parameters, compared to Li_2SiP_2, the channel size shrinks significantly due to rotation and warping of the supertetrahedra, leading to lower ionic conductivities of $1.5(3) \times 10^{-7}$ S·cm^{-1}.

The compound $LiGe_3P_3$ is isotypic to $Li_{0.9}Ge_{2.9}As_{3.1}$ and there consist identical polyanions as $NaGe_3P_3$. $LiGe_3P_3$ forms slabs of GeP_4 tetrahedra and Ge_2 dumbbells and is the first lithium phosphidotetrelate comprising formally negatively charged tetrel atoms. Although very similar polyanions are observed in various compounds they often realize different structure types. The cation size seems to have a particular effect on the structure type. The two Li containing compounds $LiGe_3P_3$ and $Li_{0.9}Ge_{2.9}As_{3.1}$ crystallize in the same structure type containing two polyanionic slabs in the unit cell, but even by replacing Li with Na in $NaGe_3P_3$ a different structure type with only one slab within the unit cell is realized. The difference in the crystal structure of $LiGe_3P_3$ compared to the so far known lithium phosphidotetrelates is also indicated by an altering macroscopic behavior. While in $LiGe_3P_3$ the electric properties are dominated by electronic conduction, an unprecedented stability in contact with water is observed. The information about the broad set of properties found in the new phosphidogermanates can help designing new generations of ionic conductors.

Experimental Section

All syntheses were carried out in an argon atmosphere in Gloveboxes (MBraun, 200B) with moisture and oxygen level below 1 ppm or in containers, which were sealed under Ar atmosphere.

Bulk Synthesis via Ball Milling and Annealing: For both compounds the synthesis route includes two steps, using lithium (Rockwood Lithium, 99 %), germanium (EVOCHEM GmbH, 99.999 %) and red phosphorus (ChemPur, 99.999 %). In the first step reactive mixtures (3 g) were prepared by mechanochemical milling using a Retsch PM100 Planetary Ball Mill (350 rpm, 36 h, 10 min interval, 3 min break) with a tungsten carbide milling jar (V = 50 mL) and three balls with a diameter of 15 mm. In the second step 300 mg fractions of the reactive mixture were pressed to pellets, sealed in a carbon coated silica glass ampoules and were annealed. To reduce the amount of side phases such as Ge, a slight excess of Li was used for synthesis of both compounds.

Single crystals of Li_2GeP_2 and $LiGe_3P_3$ were obtained by a high temperature reaction of mixtures with the element ratios for Li, Ge and P of 2:1:2 and 3:3:7, respectively. The samples (300 mg) were heated in a tantalum ampoule to 700 °C for 24 h and slowly cooled to room temperature (rate: 1 K·min^{-1}). Li_2GeP_2 crystallizes as red transparent blocks and $LiGe_3P_3$ forms black bar-shaped crystals.

For Li_2GeP_2 294.4 mg (42.4 mmol) Li, 1467.6 mg (20.2 mmol) Ge and 1251.6 mg (40.4 mmol) P were loaded into the ball mill and for the annealing process the sample was heated to 600 °C with a rate of 4 K·min^{-1} and dwelled for 24 h, afterwards slowly cooled for 24 h to 500 °C and finally cooled to room temperature with a rate of 1 K·min^{-1}.

$LiGe_3P_3$ was prepared from 70.0 mg (10.1 mmol) Li, 2057.2 mg (28.3 mmol) Ge and 877.3 mg (28.3 mmol) P. The fractions used for annealing were heated to 500 °C with a rate of 4 K·min^{-1}, dwelled for 48 h and cooled to room temperature with a rate of 1 K·min^{-1}.

Powder X-ray Diffraction: Data were collected at room temperature on a STOE Stadi P diffractometer equipped with a Ge(111) monochromator, a Cu-$K_{\alpha1}$ radiation source (λ = 1.54056 Å) and a Dectris MYTHEN 1 K detector in Debye–Scherrer setup. Samples were sealed in glass capillaries (Ø 0.3 mm) for measurement. The sample of $LiGe_3P_3$ was diluted with diamond powder to reduce X-ray absorption and all diffraction patterns were referenced against a Si standard. Raw data were processed with WinXPOW[21] software and Rietveld refinements were executed with FullProf.[22] During Rietveld refinement Li displacement parameters were kept constant and the reflections of added diamond powder were refined by profile fitting.

Single Crystal X-ray Data Collection: Single crystal of Li_2GeP_2 and $LiGe_3P_3$ were isolated and sealed in a glass capillary (0.3 mm). For diffraction data collection, the capillary was mounted on a Xcalibur3 (Oxford Diffraction, Mo-K_α radiation, λ = 0.71073) diffractometer equipped with a Sapphire 3 CCD detector and a nitrogen jet cooling system for measurements at 120 K. Structures were solved by Direct Methods (SHELXS-2014) and refined by full-matrix least-squares calculations against F^2 (SHELXL-2014).[23] Detailed information on the single crystal data collection and structural refinements are listed in Tables 1–5, further details are given in the Supporting Information.

Further details of the crystal structures investigations may be obtained from the Fachinformationszentrum Karlsruhe, 76344 Eggenstein-Leopoldshafen, Germany (Fax: +49-7247-808-666; E-Mail: crysdata@fiz-karlsruhe.de, http://www.fiz-karlsruhe.de/request for deposited data.html) on quoting the depository numbers CSD-1953470 (Li_2GeP_2, 120 K), CSD-1953471 (Li_2GeP_2, 293 K), CSD-1953472 ($LiGe_3P_3$, 120 K), and CSD-1953473 ($LiGe_3P_3$, 293 K).

Differential Scanning Calorimetry (DSC): For investigation of the thermal behavior of the compounds a Netzsch DSC 404 Pegasus device was used. Niobium crucibles were filled with 50 mg to 100 mg sample and sealed by arc-welding. Empty sealed crucibles served as reference. Measurements were performed in an argon flow of 75 mL·min^{-1} and a heating/cooling rate of 10 K·min^{-1} up to a temperature of 750 °C. Data collection and handling was carried out with the Proteus Thermal Analysis program.[24]

Solid State MAS NMR Spectroscopy: Magic angle spinning nuclear magnetic resonance (MAS NMR) spectra were recorded with a Bruker Avance 300 operating at 7.04 T. Resonance frequencies of 44.2 and 121.5 MHz and pulse widths of 6 and 1.33 µs were applied for ^{6}Li and ^{31}P measurements, respectively. For both nuclei relaxation delays of 30 s were set. Samples were diluted with Nb_2O_5 in a 1:2 ratio, packed in 4 mm ZrO_2 MAS NMR probes and rotated with frequencies of 15 kHz during the measurements. The spectra were referenced to 1 mol L^{-1} LiCl aqueous solution, solid LiCl and $(NH_4)H_2PO_4$.

Electric Conductivity Measurements: The ionic and electronic conductivities of Li_2GeP_2 and $LiGe_3P_3$ at room temperature were determined by electrochemical impedance spectroscopy (EIS) in a custom build cell. The setup consisted of two stainless-steel current collectors, a stainless-steel casing, a PEEK tube, hardened stainless-steel dies and pistons comprising a gasket for tightening the cell as well as six screws for fixing the cell. Between the two 8 mm dies powdered samples (100 mg) were loaded and the screws were fastened with a torque of 30 Nm, compressing the samples to at least 93 % of the crystal density. For the determination of the compressed pellet thickness, distances between six holes in the current collectors were measured using a precision caliper. Impedance spectra were recorded on a Bio-Logic potentiostat (SP-200) in a frequency range from 3 MHz to 50 mHz at a potentiostatic excitation of ±50 mV. Data were processed using the software EC-Lab (V 11.26). The measurements were performed in an Ar-filled glove box at 298 K. The electronic conductivity was determined with the same setup using a potentiostatic polarization applying voltages of 50, 100 and 150 mV for 16 h each. All measurements were conducted in a tempered glove box at 27(1) °C. Total conductivities obtained from impedance measurements were corrected for the electronic contribution to obtain the ionic conductivity.

Supporting Information (see footnote on the first page of this article): Details of the single crystal structure determinations at 120K and 293K, of the Rietveld refinements, of the stability experiments, and of the conductivity and DSC measurements.

Acknowledgements

The work was carried out as part of the research project ASSB coordinated by ZAE Bayern. The project is funded by the Bavarian Ministry of Economic Affairs, Regional Development and Energy. The authors greatly acknowledge *Tassilo Restle* for DSC measurements, and *Johannes Landesfeind* and *Tanja Zünd* for the design of the conductivity measurement cell.

Keywords: Ball milling; Lithium phosphidogermanates; Solid-state structures; Conducting materials; Ion conductor

References

[1] J. Janek, W. G. Zeier, *Nat. Energy* **2016**, *1*, 1.
[2] B. V. Lotsch, J. Maier, *J. Electroceram.* **2017**, *38*, 128.

[3] Z. Zhang, Y. Shao, B. V. Lotsch, Y.-S. Hu, H. Li, J. Janek, L. F. Nazar, C.-W. Nan, J. Maier, M. Armand, L. Chen, *Energy Environ. Sci.* **2018**, *11*, 1945.
[4] Y. Zhu, X. He, Y. Mo, *ACS Appl. Mater. Interfaces* **2015**, *7*, 23685.
[5] Y. Kato, S. Hori, T. Saito, K. Suzuki, M. Hirayama, A. Mitsui, M. Yonemura, H. Iba, R. Kanno, *Nat. Energy* **2016**, *1*, 16030.
[6] H.-J. Deiseroth, S.-T. Kong, H. Eckert, J. Vannahme, C. Reiner, T. Zaiß, M. Schlosser, *Angew. Chem.* **2008**, *120*, 767; *Angew. Chem. Int. Ed.* **2008**, *47*, 755.
[7] L. Toffoletti, H. Kirchhain, J. Landesfeind, W. Klein, L. van Wüllen, H. A. Gasteiger, T. F. Fässler, *Chem. Eur. J.* **2016**, *22*, 17635.
[8] A. Haffner, A.-K. Hatz, I. Moudrakovski, B. V. Lotsch, D. Johrendt, *Angew. Chem.* **2018**, *130*, 6263; *Angew. Chem. Int. Ed.* **2018**, *57*, 6155.
[9] H. Eickhoff, S. Strangmüller, W. Klein, H. Kirchhain, C. Dietrich, W. G. Zeier, L. van Wüllen, T. F. Fässler, *Chem. Mater.* **2018**, *30*, 6440.
[10] S. Strangmüller, H. Eickhoff, D. Müller, W. Klein, G. Raudaschl-Sieber, H. Kirchhain, C. Sedlmeier, V. Baran, A. Senyshyn, V. L. Deringer, L. van Wüllen, H. A. Gasteiger, T. F. Fässler, *J. Am. Chem. Soc.* **2019**, *141*, 14200–14209.
[11] H. Eickhoff, L. Toffoletti, W. Klein, G. Raudaschl-Sieber, T. F. Fässler, *Inorg. Chem.* **2017**, *56*, 6688.
[12] J. Klein, B. Eisenmann, *Mater. Res. Bull.* **1988**, *23*, 587.
[13] K. Feng, W. Yin, R. He, Z. Lin, S. Jin, J. Yao, P. Fu, Y. Wu, *Dalton Trans.* **2012**, *41*, 484.
[14] J. Mark, M. P. Hanrahan, K. E. Woo, S. Lee, A. J. Rossini, K. Kovnir, *Chem. Eur. J.* **2019**, *25*, 6392.
[15] M. Khatun, S. S. Stoyko, A. Mar, *J. Solid State Chem.* **2016**, *238*, 229.
[16] W.-M. Hurng, J. D. Corbett, S.-L. Wang, R. A. Jacobson, *Inorg. Chem.* **1987**, *26*, 2392.
[17] H.-G. von Schnering, M. Schwarz, R. Nesper, *J. Less-Common Met.* **1988**, *137*, 297.
[18] R. Juza, W. Schulz, *Z. Anorg. Allg. Chem.* **1954**, *275*, 65.
[19] M. E. Straumanis, E. Z. Aka, *J. Appl. Phys.* **1952**, *23*, 330.
[20] T. Wadsten, *Acta Chem. Scand.* **1967**, *21*, 593.
[21] *WinXPOW V3.0.2.1.*, 3.0.2.1.; STOE & Cie GmbH: Darmstadt, Germany, **2011**.
[22] J. Rodriguez-Carvajal, J. Gonzales-Platas, *FullProf Suite 2. 05*, Institute Laue-Langevin Grenoble: France, **2011**.
[23] G. M. Sheldrick, *Acta Crystallogr., Sect. C: Struct. Chem.* **2015**, *71*, 3.
[24] *Proteus Thermal Analysis V4.8.2*, Netzsch-Gerätebau GmbH: Selb, **2006**.

Received: September 13, 2019
Published Online: November 21, 2019

